

Hybrid-TTA: Continual Test-time Adaptation via Dynamic Domain Shift Detection

Hyewon Park¹, Hyejin Park¹, Jueun Ko¹, Dongbo Min¹

¹Ewha W. University
{hwpark, clrra, jueun.ko, dbmin}@ewha.ac.kr

Abstract

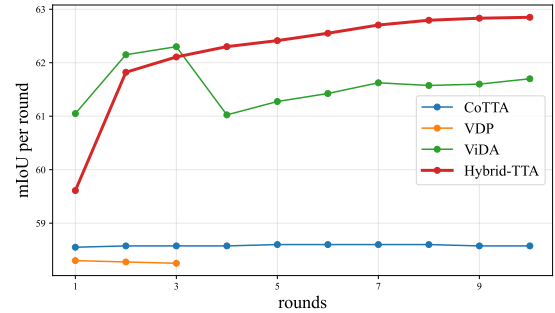
Continual Test Time Adaptation (CTTA) has emerged as a critical approach for bridging the domain gap between the controlled training environments and the real-world scenarios, enhancing model adaptability and robustness. Existing CTTA methods, typically categorized into Full-Tuning (FT) and Efficient-Tuning (ET), struggle with effectively addressing domain shifts. To overcome these challenges, we propose Hybrid-TTA, a holistic approach that dynamically selects instance-wise tuning method for optimal adaptation. Our approach introduces the Dynamic Domain Shift Detection (DDSD) strategy, which identifies domain shifts by leveraging temporal correlations in input sequences and dynamically switches between FT and ET to adapt to varying domain shifts effectively. Additionally, the Masked Image Modeling based Adaptation (MIMA) framework is integrated to ensure domain-agnostic robustness with minimal computational overhead. Our Hybrid-TTA achieves a notable 1.6%*p* improvement in mIoU on the Cityscapes-to-ACDC benchmark dataset, surpassing previous state-of-the-art methods and offering a robust solution for real-world continual adaptation challenges.

Code — <https://sites.google.com/view/hybrid-tta/>

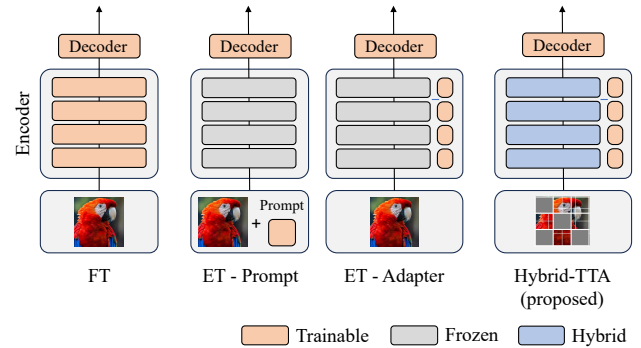
Introduction

Deep learning has gathered significant attention in computer vision due to its powerful representation capability and versatility. Despite achieving high performance on curated datasets, deep learning models face a major challenge: the gap between controlled environments and ever-changing real world. These models often struggle to maintain accuracy when faced with diverse and unpredictable scenarios. In this regard, Domain Generalization (DG) (Gulrajani and Lopez-Paz 2020; Li et al. 2018; Peng et al. 2022) and Domain Adaptation (DA) (Hoyer, Dai, and Van Gool 2022; Zou et al. 2018) focus on enhancing model robustness and adaptability to ensure reliable performance across new, unseen domains. While DG attempts to train models that generalize well to unseen domains, it has inherent limitations in adapting to continuously changing target environments, as it cannot utilize information from target datasets. On the other

Copyright © 2025, Association for the Advancement of Artificial Intelligence (www.aaai.org). All rights reserved.



(a) Performance Comparison on Cityscapes-to-ACDC



(b) Different Tuning Strategies in CTTA

Figure 1: Necessity of hybrid tuning in CTTA: (a) Performance Comparison on Cityscapes-to-ACDC over 10 rounds, showing Full-Tuning (FT) (CoTTA (Wang et al. 2022), ViDA (Liu et al. 2023)) and Efficient-Tuning (ET) (VDP (Gan et al. 2023)). (b) Graphical overview of different tuning strategies in CTTA, illustrating the distinction between FT, ET with prompts (VDP), ET with adapters (Park et al. 2023), and the proposed Hybrid-TTA approach.

hand, DA often struggles with flexibility, typically assuming a stationary target dataset, which may limit its effectiveness across multiple target domains.

Given the dynamic nature of target domains during testing, Continual Test-Time Adaptation (CTTA) has emerged

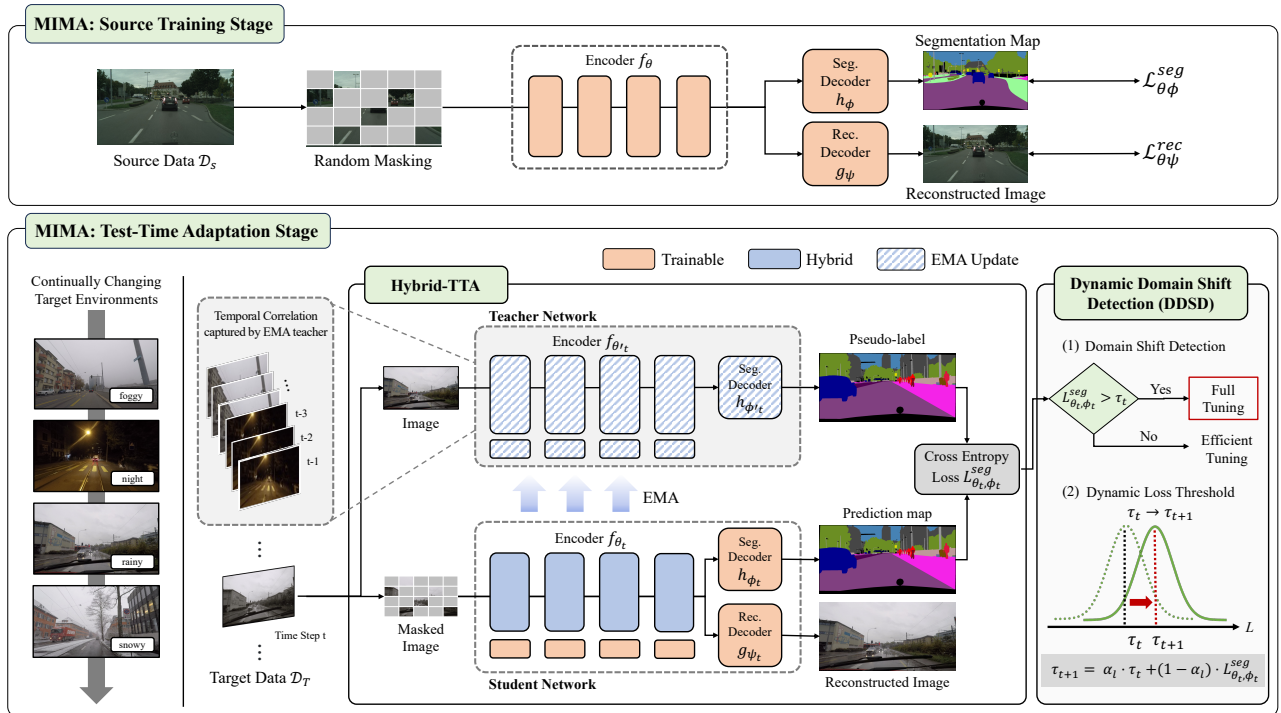


Figure 2: Overview of the **Hybrid-TTA** framework and its integration into the **Masked Image Modeling based Adaptation (MIMA)** pipeline. The top section illustrates the Source Training Stage with MIMA, where the model is trained with a masked image modeling approach to generate both segmentation maps and reconstructed images. The bottom section shows the Test-time Adaptation Stage with MIMA under continually changing target environments (e.g., foggy, night, rainy, snowy conditions). Here, **Dynamic Domain Shift Detection (DDSD)** is used along with MIMA, which detects the domain shift and switches between Efficient-Tuning and Full-Tuning via instance-wise dynamic cross-entropy loss thresholding to maintain optimal adaptation performance.

as a method, enabling models to adapt in real-time. As illustrated in Fig. 1b, existing CTTA methods are broadly categorized into two groups: (1) Full-tuning (FT), which updates all model parameters for each image (Wang et al. 2022; Liu et al. 2024) and (2) Efficient-tuning (ET), which updates only a subset of parameters (Gan et al. 2023; Song et al. 2023; Gao et al. 2022) or batch normalization (BN) parameters (Wang et al. 2020; Gong et al. 2022; Wang et al. 2023).

FT methods are known for their adaptability but come with notable drawbacks: *a) Low Efficiency*, as fully updating the model for each target image is computationally expensive, and *b) Unstable Training & Error Accumulation*, where the reliance on pseudo-labels, which is self-generated for unsupervised online learning, can introduce high randomness to the model, leading to error accumulation and performance degradation. For example, as shown in Fig. 1a, ViDA (Liu et al. 2023), a state-of-the-art FT method, demonstrates strong initial performance but experiences rapid decline due to error accumulation.

In contrast, ET methods update only a limited set of parameters, preserving source-trained knowledge and improving efficiency. This selective updating strategy introduces less randomness, resulting in more stable optimization. However, the *limited adaptability* of ET can lead to suboptimal convergence, hindering CTTA performance es-

pecially in case of significant domain shifts, as seen in VDP’s relatively poor results (Gan et al. 2023) (Fig. 1a).

Moreover, FT and ET methods share a critical limitation: their fixed number of trainable parameters for all instances can result in either excessive full tuning or insufficient tuning. This rigidity often causes the model to overlook the unique characteristics of each instance, thereby restricting the model’s ability to interact dynamically with the target dataset and ultimately leading to performance degradation.

To address these challenges, we propose **Hybrid-TTA**, a holistic approach that dynamically alternates between FT and ET based on the specific characteristics of each target instance. As depicted in Fig. 1b, Hybrid-TTA combines the adaptability of FT with the stability and efficiency of ET. By selecting appropriate tuning strategy for each instance, Hybrid-TTA ensures optimal adaptation performance across varying target conditions, making the model both flexible and stable.

Hybrid-TTA consists of two synergistic strategies: **Dynamic Domain Shift Detection (DDSD)** and **Masked Image Modeling based Adaptation (MIMA)**. DDSD determines the optimal tuning method for each incoming instance by detecting domain shifts in input images. Since domain shift occurs over time in online CTTA, our method investigates the temporal correlation among adjacent input images

by examining prediction discrepancies between the teacher and student models to identify images that are less temporally correlated. For this purpose, our method leverages weight-averaged EMA teacher model to capture temporal correlations, considering that they retain the gradual history of the input sequences (See Fig. 2. With this approach, DDS D not only maximizes the potential of the CTTA model but also minimizes its computational overhead.

MIMA is designed to leverage the generalizability and robustness of Masked Image Modeling (MIM) for CTTA. As recent studies have shown that extracting domain-agnostic features is crucial for effective CTTA (Gan et al. 2023; Liu et al. 2023), MIMA employs a multi-task based learning approach, which integrates MIM as an auxiliary task alongside the main task of semantic segmentation, to achieve this. In this framework, the model is trained simultaneously on both tasks: reconstructing masked portions of images (MIM) and performing the primary segmentation task. This dual focus encourages the model to learn shared features that are not specific to any single task, improving its ability to generalize robustly across varying target conditions. Additionally, by incorporating MIM in both source training and test-time adaptation, MIMA ensures that the model maintains its resilience throughout both stages.

Moreover, recent CTTA methods (Wang et al. 2022; Liu et al. 2023) relies on augmentation-averaged pseudo-labels to stabilize training at the cost of increased latency. However, Hybrid-TTA bypasses such augmentation strategies to reduce computational overhead during online CTTA. By leveraging MIM within MIMA, Hybrid-TTA enhances model robustness directly, minimizing reliance on additional robustness-enhancing techniques.

We summarize our main contributions as follows:

- We propose a novel Continual Test-Time Adaptation (CTTA) framework that dynamically integrates Fine-Tuning (FT) and Efficient Training (ET) to address instance-wise domain shifts. This approach optimizes online domain adaptation by selecting the most suitable tuning strategies, improving both the efficiency and effectiveness of model adaptation.
- We introduce Dynamic Domain Shift Detection (DDS D) method to detect instance-level domain shifts during test-time, by examining the prediction discrepancies between teacher and student models which represents the temporal correlation of input sequences. This method effectively identifies instances under domain shifts and guides the tuning process accordingly.
- We present Masked Image Modeling based Adaptation (MIMA), which integrates Masked Image Modeling (MIM) into a multi-task based framework, encouraging the model to extract generalized representations, achieving improved adaptation to unseen domains. This approach eliminates the need for computationally intensive augmentation-averaged pseudo-labeling strategies.

Related Work

Continual Test-Time Adaptation. Continual Test-Time Adaptation (CTTA) addresses the challenge of adapting

models in dynamic environments where target domains change over time, while traditional Test-Time Adaptation (TTA) methods assume a static target domain (Yang et al. 2021; Lim et al. 2023; Kundu et al. 2020). Recent CTTA works have employed techniques such as self-training and entropy minimization to adapt the model in an online fashion. (Wang et al. 2022) mitigates error accumulation and catastrophic forgetting using augmentation-averaged pseudo labels and stochastic weight reset, fully fine-tuning the source model for continual target domains.

Several parameter-efficient (Fu et al. 2023; Ding et al. 2023; Jo et al. 2024) CTTA methods aim to overcome catastrophic forgetting and reduce computational overhead. For example, (Song et al. 2023) uses a meta-network for stability, (Gan et al. 2023) and (Gao et al. 2022) update a small subset of parameters named visual domain prompts to improve efficiency, and (Liu et al. 2023) uses multi-rank adapters to capture the domain-agnostic and specific features. (Liu et al. 2024) employs HOG-feature reconstruction for robust adaptation, but reliance on this handcrafted module can hinder overall performance.

Strategies like those in (Wang et al. 2020), which focus on minimizing prediction entropy by training batch normalization parameters, are not discussed here due to their limited adaptability compared to FT and ET methods.

Masked Image Modeling (MIM). Masked Image Modeling (He et al. 2022; Xie et al. 2022; Choi et al. 2024a,b; Kim et al. 2024; Ahn et al. 2024; Son, Choi, and Min 2024) has gained prominence in self-supervised learning, enabling models, particularly those based on transformer architectures (Dosovitskiy et al. 2020; Liu et al. 2021; Chen et al. 2021; Ranftl, Bochkovskiy, and Koltun 2021; Lee et al. 2022, 2023), to learn robust visual representations by reconstructing masked portions of images. Notable examples include MAE (He et al. 2022) and SimMIM (Xie et al. 2022) which mask significant parts of an image and train the model to reconstruct them, learning high-quality feature representations that benefit various downstream tasks. Recently, MTO (Choi et al. 2024a) improves the efficiency of pre-training by optimizing masked tokens, whereas SBAM (Choi et al. 2024b) introduces a saliency-based adaptive masking approach, which enhances the process further by adjusting the masking ratios dynamically according to the importance of the tokens.

Building on these principles, (Hoyer et al. 2023) uses MIM in unsupervised domain adaptation (UDA) (Ganin and Lempitsky 2015; Kang et al. 2019; Cho et al. 2024) for semantic segmentation by minimizing the consistency loss between teacher’s pseudo-label from the original image and student’s prediction map from the masked image. Recent work also incorporates MIM into Test-Time Training (TTT), such as (Gandelsman et al. 2022) using MIM for both source training and test-time feature refinement in TTT, improving its adaptability to continual domain shifts.

These approaches highlight the potential of MIM-based methods in improving model robustness in dynamic environments. Our approach differs from the aforementioned methods by integrating MIM within a pseudo-multi-task frame-

work that seamlessly bridges both source training and test-time adaptation.

Proposed Method

Preliminary

Continual Test-time Adaptation (CTTA) CTTA aims to adapt a model which is initially trained on source data $\mathcal{D}_s = (\mathcal{X}_s, \mathcal{Y}_s)$, to multiple unlabeled target data distribution $\mathcal{D}_T = \{\mathcal{X}_{T_1}, \mathcal{X}_{T_2}, \dots, \mathcal{X}_{T_n}\}$ during deployment, where n represents the number of unseen domains. The entire adaptation process is constrained by two key challenges: (1) the model cannot access any source data during test-time adaptation, and (2) the model can only access each instance of target domain once, necessitating efficient and effective use of respective target instance. When the target domain data \mathcal{X}_{T_i} consists of N_i target samples for $i = 1, \dots, n$, for a simplicity of notations, we denote x_t by the t^{th} target instance for $t = 0, \dots, |\mathcal{D}_T| - 1$, where $|\mathcal{D}_T| = \sum_{i=1}^n N_i$. Similarly, in the following sections of this paper, we omit the domain notation T_1, \dots, T_n as all target domains are considered to be integrated into a single sequence.

To tackle the challenges of CTTA as an unsupervised online learning, a common strategy is to use a weight-averaged teacher model to generate pseudo-labels for the target data (Wang et al. 2022; Tarvainen and Valpola 2017). In source training, the student encoder f_θ and task decoder h_ϕ is trained on the source dataset \mathcal{D}_s , establishing the source-trained parameters θ_s, ϕ_s . During test-time, the teacher model f'_θ, h'_ϕ is firstly initialized with these parameters θ_s, ϕ_s . As the model encounters new target data over time t , the teacher model generates pseudo-labels $\hat{y}'_t = h_{\phi'_t}(f_{\theta'_t}(x_t))$ for each input x_t . The student model is then updated by minimizing the task loss $\mathcal{L}_{\theta_t, \phi_t}^{\text{seg}}$ between its own predictions \hat{y}_t and the teacher’s pseudo-labels \hat{y}'_t .

After each update of the student model, the weights of the teacher model θ', ϕ' are adjusted using an exponential moving average (EMA) (Grill et al. 2020; Chen and He 2021; Choi et al. 2023b,a) of the student’s updated weights:

$$\theta'_{t+1} = \alpha \cdot \theta'_t + (1 - \alpha) \cdot \theta_{t+1} \quad (1)$$

where α is a smoothing factor that governs the influence of the student’s weights on the teacher model’s updates. Eq. (1) applies for both θ' and ϕ' .

While this EMA-based updating strategy is a commonly used self-supervised learning technique for teacher model update in CTTA, there are several methods of tuning the main model’s parameters. Most CTTA approaches typically employ either Full-Tuning (FT) (Wang et al. 2022; Brahma and Rai 2023) or Efficient-Tuning (ET) (Gan et al. 2023; Song et al. 2023; Gao et al. 2022) strategies, where FT updates all model parameters to adapt to new target domains comprehensively, and ET focuses on selective parameter updates to balance adaptation with computational efficiency.

Masked Image Modeling For image reconstruction, SimMIM (Xie et al. 2022) is broadly utilized, where the input images are partially occluded with random patch masks and passed through the Transformer encoder, and then decoder

which is responsible for predicting the original pixels of the masked patches. In MIM (Xie et al. 2022), the training objective is typically set as

$$\min_{\theta, \psi} \mathbb{E}_{x \sim \mathcal{D}} \mathcal{L}_{\text{rec}}(x \odot M, g_\psi(z) \odot M), \quad z = f_\theta(\tilde{x}), \quad (2)$$

$$\tilde{x} = x \odot (1 - M) + e \odot M$$

where \odot represents an element-wise multiplication, and \mathcal{D} is the train data distribution. M denotes a patch mask, whose element is 1 if masked, 0 otherwise¹. $f(\cdot)$ and $g(\cdot)$ are encoder and reconstruction decoder respectively, with parameters θ and ψ , and z is the learned representation. The masked input \tilde{x} is generated by replacing the masked patches in x with trainable mask tokens e . The reconstruction loss \mathcal{L}_{rec} is computed only for masked regions.

Overview of Hybrid-TTA

We introduce the Hybrid Test-Time Adaptation (Hybrid-TTA) framework, specifically designed for Continual Test-Time Adaptation (CTTA), as illustrated in Fig. 2. To effectively manage the wide range of domain gaps presented by continuously changing instances, a CTTA model needs to be both adaptable to new domains and stable within familiar ones. Hybrid-TTA achieves this by dynamically alternating between two tuning strategies: Full-Tuning (FT) and Efficient-Tuning (ET).

At the core of Hybrid-TTA is the Dynamic Domain Shift Detection (DDSD) module, which determines when a new input exhibits a significant domain shift. Once such a shift is detected, the framework triggers FT, allowing for comprehensive model adaptation by updating all parameters. In contrast, when domain shifts are minimal, ET selectively updates only a subset of parameters, ensuring computational efficiency and maintaining stability.

Additionally, we incorporate Masked Image Modeling-based Adaptation (MIMA), which helps the model learn robust, task-agnostic features through a multi-task based learning approach (Zhang and Yang 2021; Liu, Johns, and Davison 2019; Kim, Choi, and Min 2022; Kim, Choi, and Min). By integrating MIMA into both the initial source training and the test-time adaptation stages, the framework enables the model to be resilient to the continual domain shifts characteristics of CTTA.

Dynamic Domain Shift Detection (DDSD)

To effectively detect domain shifts, DDSD module leverages the weight-averaged teacher model employing exponential moving average (EMA). Unlike the student model, which undergoes rapid updates with each new instance, the teacher model’s weights change more gradually, enabling it to capture temporal correlations within the evolving target image sequence. As described in Fig. 2, while the student model updates with each new image at time t , the teacher model’s weights are influenced by multiple preceding images, effectively retaining a history of prior adaptations. In essence, the teacher model serves as a memory buffer, capturing and maintaining information from past images.

¹ $x \odot (1 - M)$ represents “visible patches” and vice versa.

Therefore, when an input image experiences a domain shift, the pseudo labels generated by the teacher model is likely to differ from the student model’s predictions. This is because the teacher model is more adhesive to its previous state, while the student model is more responsive to recent changes. This discrepancy is a strong indicator of a domain shift. Upon detecting such a shift, the DDS module dynamically triggers the appropriate tuning strategy to selectively update only the most relevant parameters to ensure efficiency: DDS module employ FT for significant discrepancy to comprehensively adapt the model to the new domain. Conversely, the DDS module opts for ET if the discrepancy is minimal, indicating a minor domain shift.

Loss Thresholding Strategy. Leveraging this characteristic, we detect domain shifts by comparing pseudo labels and prediction maps using a cross-entropy loss and dynamically thresholding the segmentation loss, inspired by (Yang et al. 2023; Choi et al. 2021).

An initial loss threshold τ_0 is set to 0, under the assumption that all upcoming instances may be under domain shift. At each time step t , this threshold is updated using an EMA of the newly calculated loss:

$$\tau_{t+1} = \alpha_l \cdot \tau_t + (1 - \alpha_l) \cdot \mathcal{L}_{\theta_t, \phi_t}^{seg} \quad (3)$$

where α_l is another smoothing factor for the EMA of loss threshold. $\mathcal{L}_{\theta_t, \phi_t}^{seg}$ is a segmentation loss, which is calculated between the teacher’s pseudo label and the student’s prediction map at time step t . If the loss value for the input image at time t exceeds the threshold τ , i.e. $\mathcal{L}_{\theta_t, \phi_t}^{seg} > \tau_t$, a domain shift is detected, FT is applied, and vice versa.

MIM based Adaptation (MIMA)

Test-time adaptation in our framework consists of two distinct stages: (1) *Source Training* stage, where the model is initially trained on the source dataset, and (2) *Test-Time Adaptation* stage, which occurs on the target dataset during deployment. To seamlessly bridge these stages and enhance adaptability, we employ a multi-task based architecture that combines two learning tasks: semantic segmentation and masked image reconstruction using Masked Image Modeling (MIM). This architecture is applied consistently across both stages to ensure coherence and continuity in learning. A similar approach, TTT-MAE (Gandelsman et al. 2022), adopts MIM in a separated manner from the main task and resets the source model after each instance, limiting its ability to leverage previously encountered target data for further updates. In contrast, MIMA is specifically designed to handle continuous domain shifts. By leveraging all encountered target instances and integrating both reconstruction and segmentation consistently across the source training and test-time adaptation stages, MIMA generates robust pseudo-labels, enhancing adaptation performance.

Source Training Stage. In this stage, the model is trained by supervised learning on the source dataset within a multi-task based architecture that incorporates both segmentation and reconstruction tasks. Each input image is partially masked and then passed through the encoder f for feature

extraction. The resulting features are then simultaneously processed by two decoders: a reconstruction decoder g and a segmentation decoder h . The segmentation output is compared to the ground truth, while the reconstructed image is compared to the original input.

For reconstruction, the model aims to reconstruct the original image from the masked input \tilde{x} based on Eq. (2). The reconstruction is optimized using $L1$ loss, as below:

$$\mathcal{L}_{\theta, \psi}^{rec} = \frac{1}{|M|} \| (x - g_\psi(f_\theta(\tilde{x}))) \odot M \|_1, \quad (4)$$

where $x, g_\psi(f_\theta(\tilde{x})) \in \mathbb{R}^{3HW \times 1}$ represent the input image and predicted image. Since M denotes the patch mask in Eq. (2), $|M|$ indicates the number of masked pixels.

For segmentation, cross-entropy loss is computed as:

$$\mathcal{L}_{\theta, \phi}^{seg} = \mathcal{CE}(y, h_\phi(f_\theta(\tilde{x}))), \quad (5)$$

where y represents the supervised label, and $h(f(\tilde{x}))$ denotes the prediction map made by the student model. Note that f and h also use the masked input image \tilde{x} mentioned in Eq. (2). The total loss for source training stage is given by:

$$\mathcal{L}_{total} = \mathcal{L}_{\theta, \phi}^{seg} + \mathcal{L}_{\theta, \psi}^{rec} \quad (6)$$

Test-Time Adaptation Stage. As illustrated in Fig. 2, during test-time adaptation, the teacher model takes the original image as input to generate pseudo-labels. The same image is then masked and fed into the student model’s feature extraction encoder to create a masked image representation. This representation is subsequently passed through the decoders used in the source training stage, producing both a prediction map and a reconstructed image. At time step t , the reconstruction loss between the original and reconstructed images is calculated as in source training stage (Eq. (4)). However, the segmentation loss is now computed between the teacher’s pseudo-labels and the student’s predictions as following:

$$\mathcal{L}_{\theta_t, \phi_t}^{seg} = \mathcal{CE}(\hat{y}_t, h_{\phi_t}(f_{\theta_t}(\tilde{x}_t))), \quad (7)$$

where $\hat{y}_t = h_{\phi'}(f_{\theta'}(x_t))$ represents the pseudo-label generated by the teacher model. The final loss is computed as in Eq. (6) and updated at each time t , as the model continually adapts during TTA process.

Experiments

Experimental Setups

Dataset and Task Setup. We follow (Wang et al. 2022) experimental setup for segmentation CTTA using the Cityscape-to-ACDC (Corrts et al. 2016; Sakaridis, Dai, and Van Gool 2021) benchmarks which assesses test-time segmentation performance under four weather conditions—Fog, Night, Rain, and Snow—repeated cyclicly for ten times for long-term adaptation evaluation. Although our method is primarily designed for semantic segmentation, we also test our method on ImageNet-to-ImageNet-C (Hendrycks and Dietterich 2019) benchmark for classification, adapting to 15 corruption types with severity level 5. We report results using mean intersection over union (mIoU) metric for segmentation and error rate (%) for classification.

Table 1: **Performance comparison of Segmentation CTTA baselines on Cityscapes-to-ACDC benchmark.** Mean is the average score of mIoU. The best results are highlighted in **bold**. VDP and SVDP performance from round 4 to 10 are omitted due to unavailability of the official results.

Test Condition	1				4				7				10				All ↑ Mean
	Fog	Night	Rain	Snow	Fog	Night	Rain	Snow	Fog	Night	Rain	Snow	Fog	Night	Rain	Snow	
Source	69.1	40.3	59.7	57.8	69.1	40.3	59.7	57.8	69.1	40.3	59.7	57.8	69.1	40.3	59.7	57.8	56.7
BN Stats Adapt (Schneider et al. 2020)	62.3	38.0	54.6	53.0	62.3	38.0	54.6	53.0	62.3	38.0	54.6	53.0	62.3	38.0	54.6	53.0	52.0
TENT-continual (Wang et al. 2020)	69.0	40.2	60.1	57.3	66.5	36.3	58.7	55.0	64.2	32.8	55.3	50.9	61.8	29.8	51.9	47.8	52.3
CoTTA (Wang et al. 2022)	70.9	41.2	62.4	59.7	70.9	41.0	62.7	59.7	70.9	41.0	62.8	59.7	70.9	41.0	62.8	59.7	58.6
EcoTTA (Song et al. 2023)	68.5	35.8	62.1	57.4	68.1	35.3	62.3	57.3	67.2	34.2	62.0	56.9	66.4	33.2	61.3	56.3	55.2
VDP (Gan et al. 2023)	70.5	41.1	62.1	59.5	-	-	-	-	-	-	-	-	-	-	-	-	58.3
SVDP (Yang et al. 2024)	72.1	44.0	65.2	63.0	-	-	-	-	-	-	-	-	-	-	-	-	61.1
ViDA (Liu et al. 2023)	71.6	43.2	66.0	63.4	70.9	44.0	66.0	63.2	72.3	44.8	66.5	62.9	72.2	45.2	66.5	62.9	61.6
Hybrid-TTA (ours)	69.1	43.4	62.8	63.2	70.8	49.7	65.7	62.9	70.6	51.1	65.9	63.3	70.3	51.6	66.0	63.5	62.2



Figure 3: **Qualitative comparison of segmentation results on Night domain for Cityscapes-to-ACDC benchmark.**

Baselines. We first compare our method with the state-of-the-art approaches, which can be divided into two categories: Full Tuning (FT) methods such as CoTTA (Wang et al. 2022), ViDA (Liu et al. 2023), SVDP (Yang et al. 2024); Efficient Tuning (ET) methods including VDP (Gan et al. 2023), EcoTTA (Song et al. 2023).

Implementation Details. We follow the setups from prior work (Wang et al. 2022). For segmentation CTTA, we use SegFormer-B5 (Xie et al. 2021) trained on down-sampled Cityscapes (1024×1024) and test it on ACDC (960×544). For classification CTTA, we use ViT-base (Dosovitskiy et al. 2020) trained on ImageNet1k with SimMIM (Xie et al. 2022), using 224×224 images for both datasets. To implement Efficient Tuning, we incorporate AdaptMLP (Chen et al. 2022) in each transformer layer which occupies 10% of the overall parameters (see Fig. 1). All experiments are conducted using NVIDIA A100, A6000, and RTX3090. Further details are in the supplementary material.

Experiments on Segmentation CTTA

As shown in Tab. 1 and Fig. 1a, our approach outperforms existing CTTA methods, including both FT and ET techniques. The performance of BN Stats Adapt and TENT-Continual declines gradually due to catastrophic forgetting. Similarly, EcoTTA, a CNN based ET method, shows slight degradation due to catastrophic forgetting and insufficient adaptability. CoTTA maintain stable performance by preventing error accumulation with augmentation-averaged pseudo-labels, but fails to extract domain-agnostic features, leading to only modest gains.

Our approach remains competitive with state-of-the-art

methods like ViDA. Notably, as Fig. 1a shows, our method consistently improves over time, achieving significant performance gains of +1.2%p, +8.2%p, +3.2%p, +0.3%p in the Fog, Night, Rain, Snow domains, respectively. In contrast, ViDA’s performance is less stable due to error accumulation. This highlights the effectiveness of the DDS module in Hybrid-TTA, which dynamically selects the appropriate adaptation strategy for each instance, successfully mitigating impact of error accumulation.

Furthermore, Hybrid-TTA shows the most significant improvement in the Night domain, typically the most challenging domain due to poor lighting condition and significant differences in object appearances. As seen in Fig. 3, Hybrid-TTA generates better inference results than other methods. This success is attributed to the MIMA module, which effectively captures domain-agnostic features across both the source domain and multiple target domains.

Experiments on Classification CTTA

Though initially designed for semantic segmentation, Hybrid-TTA was also evaluated for image classification to test its versatility. As shown in Tab. 2, Hybrid-TTA performs competitively compared to other CTTA methods. Especially, the comparison with TTT-MAE suggests the benefits of MIMA, a multitask-based approach tailored specifically to the downstream task. Notably, recent CTTA methods such as CoTTA, ViDA, and Continual-MAE rely on multi-scale augmentation to enhance pseudo-label reliability, resulting in significant computational overhead due to multiple inferences for augmented images. In contrast, Hybrid-TTA achieves superior mIoU and frame rate without employing augmentation-averaging, as evidenced by the latency analy-

Table 2: **Classification error rate(%) for ImageNet-to-ImageNet-C benchmark.** The best results are highlighted in **bold**.

Method	gaus.	shot	impu.	defo.	glas.	moti.	zoom	snow	fros.	fog	brig.	cont.	elas.	pixe.	jpeg.	Mean ↓
Source	53.0	51.8	52.1	68.5	78.8	58.5	63.3	49.9	54.2	57.7	26.4	91.4	57.5	38.0	36.2	55.8
TENT (Wang et al. 2020)	52.2	48.9	49.2	65.8	73.0	54.5	58.4	44.0	47.7	50.3	23.9	72.8	55.7	34.4	33.9	51.0
CoTTA (Wang et al. 2022)	52.9	51.6	51.4	68.3	78.1	57.1	62.0	48.2	52.7	55.3	25.9	90.0	56.4	36.4	35.2	54.8
TTT-MAE (Gandelsman et al. 2022)	74.9	73.0	73.0	68.3	74.9	60.5	57.1	62.1	53.7	57.2	32.3	90.8	54.5	40.1	40.1	60.8
VDP (Gan et al. 2023)	52.7	51.6	50.1	58.1	70.2	56.1	58.1	42.1	46.1	45.8	23.6	70.4	54.9	34.5	36.1	50.0
Hybrid-TTA (ours)	54.4	49.6	49.4	63.4	69.4	53.2	60.9	44.7	47.1	47.8	25.8	88.1	52.0	36.2	33.2	51.7

Table 3: **Effectiveness of each proposed components.** DDS D represents the experiment where DDS D participated in selecting optimal tuning methods. Gain denotes the performance gain between two adjacent experiments. Total gain represents the performance gain between (f) and (a).

	ET	FT	DDS D	MIMA	Mean	Gain
(a)	✓				56.9	
(b)	✓			✓	58.2	+1.3%p
(c)		✓			58.6	
(d)		✓		✓	61.3	+2.7%p
(e)			✓		59.3	
(f) - ours			✓	✓	62.2	+2.9%p
Total Gain: (f) - (a)						+5.3%p

sis in Tab. 5, accomplishing both effectiveness and efficiency in CTTA process.

Ablation Studies

Effectiveness of Individual Component. We conducted ablation experiments on Cityscapes-to-ACDC to evaluate the contributions of different components in our approach. As shown in Tab. 3, the first four experiments (a-d) demonstrate the impact of the MIMA module on both vanilla ET and FT methods. The results indicates that randomly masking input images improves segmentation performance in Hybrid-TTA, with gains of +1.3%p for ET and +2.7%p for FT. The effect of MIMA is more significant in FT, suggesting that leveraging auxiliary reconstruction task during test-time enhances the model’s domain generalization ability.

In experiments (e-f), we examine the DDS D module, which dynamically selects ET or FT for each image. The combination of DDS D and MIMA yields better segmentation performance than DDS D alone, highlighting their synergistic effect. When both modules, the final performance reaches 62.2%, a 5.3%p improvement overall. In contrast, DDS D alone achieves 59.3%, 2.9%p below the best performance. These findings confirm that incorporating an auxiliary reconstruction task in CTTA helps the model learn robust, domain-agnostic knowledge, enabling better retention of previous domain knowledge through dynamic tuning.

Chronological Utilization Ratio of DDS D. Tab. 4 shows the chronological utilization ratio of FT and ET over 10-round experiments of Cityscapes-to-ACDC benchmark. Each round contains 400 images for 4 domains, 1,600 im-

Table 4: **Chronological Utilization Ratio(%) of DDS D.** The utilization ratio of FT and ET during 10-round experiments of Cityscapes-to-ACDC benchmark. Each round contains 1,600 images.

Round	1	4	7	10
FT (%)	76.8	40.3	42.6	41.8
ET (%)	23.2	59.7	57.4	58.2

Table 5: **Average Frame Rate (fps).** The average frame rate during 3 round experiments of Cityscapes-to-ACDC benchmark based on the use of augmentation-averaging pseudo-label strategy.

Method	CoTTA	SVDP	Hybrid-TTA
mIoU (%)	58.6	61.1	62.2
Frame rate (fps ↑)	0.058	0.043	1.16

ages in total. Initially, FT dominates round 1 with 76.8% usage, as most inputs are unfamiliar to the model. However, as the experiment progresses and the model adapts to previously seen domains, ET gradually becomes more prevalent, accounting for nearly 60% of inputs by the final round.

Average Frame Rate Comparison. We compare the latency of various CTTA methods by measuring average frame rate based on the use of augmentation-averaging pseudo-label strategy, as shown in Tab. 5. Since reducing adaptation latency is crucial in online learning, Hybrid-TTA avoid test-time augmentations. Unlike CoTTA and SVDP(Yang et al. 2024), which are both FT methods requiring 14 forward passes per image for multi-scale flip augmentations to generate pseudo-labels, Hybrid-TTA performs only one forward pass, achieving an average frame rate nearly 20 times higher. Despite this efficiency, Hybrid-TTA delivers the highest performance of 62.2% among the compared methods. Note that ViDA’s FPS is not reported since its segmentation source code is currently unavailable, though it uses a similar augmentation strategy as CoTTA and SVDP. All experiments are conducted under the same conditions, with only MIMA is used in Hybrid-TTA (excluding DDS D) to independently assess the impact of MIMA.

Conclusion

In this paper, we have proposed Hybrid-TTA that dynamically selects the proper tuning method for each input instance by leveraging EMA-updated teacher models. This framework promotes the interaction between the model and continually changing input sequences on target domain, resulting in improved performance. By integrating Masked Image Modeling into a multi-task based learning paradigm, our model extracts generalized features and maintains robustness across domains. Experiments on Cityscapes-to-ACDC and ImageNet-to-ImageNet-C benchmarks demonstrate that our method achieves outstanding performance in semantic segmentation with significantly reduced computational overhead. In this regard, it is expected that our hybrid framework provides new insights on developing reliable techniques for continual TTA.

Limitations. While Hybrid-TTA excels in semantic segmentation, its performance in image classification tasks, though competitive, highlights the need for further refinement. The reliance on MIM may introduce constraints in some classification scenarios, suggesting room for integrating additional techniques to enhance generalization across diverse tasks without compromising the model’s efficiency.

References

- Ahn, J.; Choi, H.; Kim, S.; and Min, D. 2024. MaDis-Stereo: Enhanced Stereo Matching via Distilled Masked Image Modeling. *arXiv preprint arXiv:2409.02846*.
- Brahma, D.; and Rai, P. 2023. A probabilistic framework for lifelong test-time adaptation. In *Proceedings of the IEEE/CVF Conference on Computer Vision and Pattern Recognition*, 3582–3591.
- Chen, H.; Wang, Y.; Guo, T.; Xu, C.; Deng, Y.; Liu, Z.; Ma, S.; Xu, C.; Xu, C.; and Gao, W. 2021. Pre-trained image processing transformer. In *Proceedings of the IEEE/CVF conference on computer vision and pattern recognition*, 12299–12310.
- Chen, S.; Ge, C.; Tong, Z.; Wang, J.; Song, Y.; Wang, J.; and Luo, P. 2022. Adaptformer: Adapting vision transformers for scalable visual recognition. *Advances in Neural Information Processing Systems*, 35: 16664–16678.
- Chen, X.; and He, K. 2021. Exploring simple siamese representation learning. In *Proceedings of the IEEE/CVF conference on computer vision and pattern recognition*, 15750–15758.
- Cho, M.; Choi, H.; Jo, H.; and Min, D. 2024. CLDA: Collaborative Learning for Enhanced Unsupervised Domain Adaptation. *arXiv preprint arXiv:2409.02699*.
- Choi, H.; Lee, H.; Jeong, S.; and Min, D. 2023a. Environment Agnostic Representation for Visual Reinforcement learning. In *Proceedings of the IEEE/CVF International Conference on Computer Vision*, 263–273.
- Choi, H.; Lee, H.; Joung, S.; Park, H.; Kim, J.; and Min, D. 2024a. Emerging Property of Masked Token for Effective Pre-training. *arXiv preprint arXiv:2404.08330*.
- Choi, H.; Lee, H.; Kim, S.; Kim, S.; Kim, S.; Sohn, K.; and Min, D. 2021. Adaptive confidence thresholding for monocular depth estimation. In *Proceedings of the IEEE/CVF International Conference on Computer Vision*, 12808–12818.
- Choi, H.; Lee, H.; Song, W.; Jeon, S.; Sohn, K.; and Min, D. 2023b. Local-Guided Global: Paired Similarity Representation for Visual Reinforcement Learning. In *Proceedings of the IEEE/CVF Conference on Computer Vision and Pattern Recognition*, 15072–15082.
- Choi, H.; Park, H.; Yi, K. M.; Cha, S.; and Min, D. 2024b. Saliency-Based Adaptive Masking: Revisiting Token Dynamics for Enhanced Pre-training. *arXiv preprint arXiv:2404.08327*.
- Cordts, M.; Omran, M.; Ramos, S.; Rehfeld, T.; Enzweiler, M.; Benenson, R.; Franke, U.; Roth, S.; and Schiele, B. 2016. The cityscapes dataset for semantic urban scene understanding. In *Proceedings of the IEEE conference on computer vision and pattern recognition*, 3213–3223.
- Ding, N.; Qin, Y.; Yang, G.; Wei, F.; Yang, Z.; Su, Y.; Hu, S.; Chen, Y.; Chan, C.-M.; Chen, W.; et al. 2023. Parameter-efficient fine-tuning of large-scale pre-trained language models. *Nature Machine Intelligence*, 5(3): 220–235.
- Dosovitskiy, A.; Beyer, L.; Kolesnikov, A.; Weissenborn, D.; Zhai, X.; Unterthiner, T.; Dehghani, M.; Minderer, M.; Heigold, G.; Gelly, S.; et al. 2020. An image is worth 16x16 words: Transformers for image recognition at scale. *arXiv preprint arXiv:2010.11929*.
- Fu, Z.; Yang, H.; So, A. M.-C.; Lam, W.; Bing, L.; and Collier, N. 2023. On the effectiveness of parameter-efficient fine-tuning. In *Proceedings of the AAAI conference on artificial intelligence*, volume 37, 12799–12807.
- Gan, Y.; Bai, Y.; Lou, Y.; Ma, X.; Zhang, R.; Shi, N.; and Luo, L. 2023. Decorate the newcomers: Visual domain prompt for continual test time adaptation. In *Proceedings of the AAAI Conference on Artificial Intelligence*, volume 37, 7595–7603.
- Gandelsman, Y.; Sun, Y.; Chen, X.; and Efros, A. 2022. Test-time training with masked autoencoders. *Advances in Neural Information Processing Systems*, 35: 29374–29385.
- Ganin, Y.; and Lempitsky, V. 2015. Unsupervised domain adaptation by backpropagation. In *International conference on machine learning*, 1180–1189. PMLR.
- Gao, Y.; Shi, X.; Zhu, Y.; Wang, H.; Tang, Z.; Zhou, X.; Li, M.; and Metaxas, D. N. 2022. Visual prompt tuning for test-time domain adaptation. *arXiv preprint arXiv:2210.04831*.
- Gong, T.; Jeong, J.; Kim, T.; Kim, Y.; Shin, J.; and Lee, S.-J. 2022. Note: Robust continual test-time adaptation against temporal correlation. *Advances in Neural Information Processing Systems*, 35: 27253–27266.
- Grill, J.-B.; Strub, F.; Altché, F.; Tallec, C.; Richemond, P.; Buchatskaya, E.; Doersch, C.; Avila Pires, B.; Guo, Z.; Gheshlaghi Azar, M.; et al. 2020. Bootstrap your own latent: a new approach to self-supervised learning. *Advances in neural information processing systems*, 33: 21271–21284.
- Gulrajani, I.; and Lopez-Paz, D. 2020. In search of lost domain generalization. *arXiv preprint arXiv:2007.01434*.

- He, K.; Chen, X.; Xie, S.; Li, Y.; Dollár, P.; and Girshick, R. 2022. Masked autoencoders are scalable vision learners. In *Proceedings of the IEEE/CVF conference on computer vision and pattern recognition*, 16000–16009.
- Hendrycks, D.; and Dietterich, T. 2019. Benchmarking neural network robustness to common corruptions and perturbations. *arXiv preprint arXiv:1903.12261*.
- Hoyer, L.; Dai, D.; and Van Gool, L. 2022. Daformer: Improving network architectures and training strategies for domain-adaptive semantic segmentation. In *Proceedings of the IEEE/CVF conference on computer vision and pattern recognition*, 9924–9935.
- Hoyer, L.; Dai, D.; Wang, H.; and Van Gool, L. 2023. MIC: Masked image consistency for context-enhanced domain adaptation. In *Proceedings of the IEEE/CVF conference on computer vision and pattern recognition*, 11721–11732.
- Jo, H.; Choi, H.; Cho, M.; and Min, D. 2024. iConFormer: Dynamic Parameter-Efficient Tuning with Input-Conditioned Adaptation. *arXiv preprint arXiv:2409.02838*.
- Kang, G.; Jiang, L.; Yang, Y.; and Hauptmann, A. G. 2019. Contrastive adaptation network for unsupervised domain adaptation. In *Proceedings of the IEEE/CVF conference on computer vision and pattern recognition*, 4893–4902.
- Kim, S.; Choi, H.; Ahn, J.; and Min, D. 2024. UniTT-Stereo: Unified Training of Transformer for Enhanced Stereo Matching. *arXiv preprint arXiv:2409.02545*.
- Kim, S.; Choi, H.; and Min, D. ????. Pseudo Label-Guided Multi Task Learning for Scene Understanding.
- Kim, S.; Choi, H.; and Min, D. 2022. Sequential cross attention based multi-task learning. In *2022 IEEE International Conference on Image Processing (ICIP)*, 2311–2315. IEEE.
- Kundu, J. N.; Venkat, N.; Babu, R. V.; et al. 2020. Universal source-free domain adaptation. In *Proceedings of the IEEE/CVF conference on computer vision and pattern recognition*, 4544–4553.
- Lee, H.; Choi, H.; Sohn, K.; and Min, D. 2022. Knn local attention for image restoration. In *Proceedings of the IEEE/CVF conference on computer vision and pattern recognition*, 2139–2149.
- Lee, H.; Choi, H.; Sohn, K.; and Min, D. 2023. Cross-scale KNN image transformer for image restoration. *IEEE Access*, 11: 13013–13027.
- Li, H.; Pan, S. J.; Wang, S.; and Kot, A. C. 2018. Domain generalization with adversarial feature learning. In *Proceedings of the IEEE conference on computer vision and pattern recognition*, 5400–5409.
- Lim, H.; Kim, B.; Choo, J.; and Choi, S. 2023. TTN: A domain-shift aware batch normalization in test-time adaptation. *arXiv preprint arXiv:2302.05155*.
- Liu, J.; Xu, R.; Yang, S.; Zhang, R.; Zhang, Q.; Chen, Z.; Guo, Y.; and Zhang, S. 2024. Continual-MAE: Adaptive Distribution Masked Autoencoders for Continual Test-Time Adaptation. In *Proceedings of the IEEE/CVF Conference on Computer Vision and Pattern Recognition*, 28653–28663.
- Liu, J.; Yang, S.; Jia, P.; Zhang, R.; Lu, M.; Guo, Y.; Xue, W.; and Zhang, S. 2023. Vida: Homeostatic visual domain adapter for continual test time adaptation. *arXiv preprint arXiv:2306.04344*.
- Liu, S.; Johns, E.; and Davison, A. J. 2019. End-to-end multi-task learning with attention. In *Proceedings of the IEEE/CVF conference on computer vision and pattern recognition*, 1871–1880.
- Liu, Z.; Lin, Y.; Cao, Y.; Hu, H.; Wei, Y.; Zhang, Z.; Lin, S.; and Guo, B. 2021. Swin transformer: Hierarchical vision transformer using shifted windows. In *Proceedings of the IEEE/CVF international conference on computer vision*, 10012–10022.
- Park, S.; Yang, S.; Choo, J.; and Yun, S. 2023. Label shift adapter for test-time adaptation under covariate and label shifts. In *Proceedings of the IEEE/CVF International Conference on Computer Vision*, 16421–16431.
- Peng, D.; Lei, Y.; Hayat, M.; Guo, Y.; and Li, W. 2022. Semantic-aware domain generalized segmentation. In *Proceedings of the IEEE/CVF conference on computer vision and pattern recognition*, 2594–2605.
- Ranftl, R.; Bochkovskiy, A.; and Koltun, V. 2021. Vision transformers for dense prediction. In *Proceedings of the IEEE/CVF international conference on computer vision*, 12179–12188.
- Sakaridis, C.; Dai, D.; and Van Gool, L. 2021. ACDC: The adverse conditions dataset with correspondences for semantic driving scene understanding. In *Proceedings of the IEEE/CVF International Conference on Computer Vision*, 10765–10775.
- Schneider, S.; Rusak, E.; Eck, L.; Bringmann, O.; Brendel, W.; and Bethge, M. 2020. Improving robustness against common corruptions by covariate shift adaptation. *Advances in neural information processing systems*, 33: 11539–11551.
- Son, S.; Choi, H.; and Min, D. 2024. SG-MIM: Structured Knowledge Guided Efficient Pre-training for Dense Prediction. *arXiv preprint arXiv:2409.02513*.
- Song, J.; Lee, J.; Kweon, I. S.; and Choi, S. 2023. Ecotta: Memory-efficient continual test-time adaptation via self-distilled regularization. In *Proceedings of the IEEE/CVF Conference on Computer Vision and Pattern Recognition*, 11920–11929.
- Tarvainen, A.; and Valpola, H. 2017. Mean teachers are better role models: Weight-averaged consistency targets improve semi-supervised deep learning results. *Advances in neural information processing systems*, 30.
- Wang, D.; Shelhamer, E.; Liu, S.; Olshausen, B.; and Darrell, T. 2020. Tent: Fully test-time adaptation by entropy minimization. *arXiv preprint arXiv:2006.10726*.
- Wang, Q.; Fink, O.; Van Gool, L.; and Dai, D. 2022. Continual test-time domain adaptation. In *Proceedings of the IEEE/CVF Conference on Computer Vision and Pattern Recognition*, 7201–7211.
- Wang, W.; Zhong, Z.; Wang, W.; Chen, X.; Ling, C.; Wang, B.; and Sebe, N. 2023. Dynamically instance-guided adaptation: A backward-free approach for test-time domain adaptive semantic segmentation. In *Proceedings of the IEEE/CVF Conference on Computer Vision and Pattern Recognition*, 24090–24099.

- Xie, E.; Wang, W.; Yu, Z.; Anandkumar, A.; Alvarez, J. M.; and Luo, P. 2021. SegFormer: Simple and efficient design for semantic segmentation with transformers. *Advances in Neural Information Processing Systems*, 34: 12077–12090.
- Xie, Z.; Zhang, Z.; Cao, Y.; Lin, Y.; Bao, J.; Yao, Z.; Dai, Q.; and Hu, H. 2022. Simmim: A simple framework for masked image modeling. In *Proceedings of the IEEE/CVF conference on computer vision and pattern recognition*, 9653–9663.
- Yang, H.; Jin, Y.-Z.; Li, Z.-Y.; Wang, D.-B.; Geng, X.; and Zhang, M.-L. 2023. Learning from noisy labels via dynamic loss thresholding. *IEEE Transactions on Knowledge and Data Engineering*.
- Yang, S.; Wang, Y.; Van De Weijer, J.; Herranz, L.; and Jui, S. 2021. Generalized source-free domain adaptation. In *Proceedings of the IEEE/CVF international conference on computer vision*, 8978–8987.
- Yang, S.; Wu, J.; Liu, J.; Li, X.; Zhang, Q.; Pan, M.; Gan, Y.; Chen, Z.; and Zhang, S. 2024. Exploring sparse visual prompt for domain adaptive dense prediction. In *Proceedings of the AAAI Conference on Artificial Intelligence*, volume 38, 16334–16342.
- Zhang, Y.; and Yang, Q. 2021. A survey on multi-task learning. *IEEE transactions on knowledge and data engineering*, 34(12): 5586–5609.
- Zou, Y.; Yu, Z.; Kumar, B.; and Wang, J. 2018. Unsupervised domain adaptation for semantic segmentation via class-balanced self-training. In *Proceedings of the European conference on computer vision (ECCV)*, 289–305.